

Regiodivergent Nucleophilic Fluorination under Hydrogen Bonding Catalysis: A Computational and Experimental Study

Matthew A. Horwitz,^{*,||} Alexander B. Dürr,^{*,||} Konstantinos Afratis,^{||} Zijun Chen,^{||} Julia Soika, Kirsten E. Christensen, Makoto Fushimi, Robert S. Paton,^{*} and Véronique Gouverneur^{*}Cite This: *J. Am. Chem. Soc.* 2023, 145, 9708–9717

Read Online

ACCESS |



Metrics & More

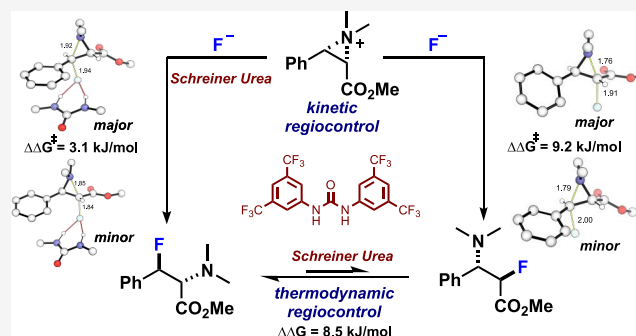


Article Recommendations



Supporting Information

ABSTRACT: The controlled programming of regiochemical outcomes in nucleophilic fluorination reactions with alkali metal fluoride is a problem yet to be solved. Herein, two synergistic approaches exploiting hydrogen bonding catalysis are presented. First, we demonstrate that modulating the charge density of fluoride with a hydrogen-bond donor urea catalyst directly influences the kinetic regioselectivity in the fluorination of dissymmetric aziridinium salts with aryl and ester substituents. Moreover, we report a urea-catalyzed formal dyotropic rearrangement, a thermodynamically controlled regiochemical editing process consisting of C–F bond scission followed by fluoride rebound. These findings offer a route to access enantioenriched fluoroamine regioisomers from a single chloroamine precursor, and more generally, new opportunities in regiodivergent asymmetric (bis)urea-based organocatalysis.



INTRODUCTION

The development and widespread application of asymmetric organocatalysis was recognized with the Nobel Prize in Chemistry awarded in 2021 to List and MacMillan.¹ Organocatalysts were also deployed to control regioselectivity including examples of asymmetric regiodivergent reactions.² Standout examples are the development of the regiocontrolled *N*-alkylation of triazoles with an amidinium hydrogen-bond donor (HBD) catalyst³ and an asymmetric regiodivergent cycloaddition catalyzed by an *N*-heterocyclic carbene leading to regioisomeric dihydroisoquinolines.⁴

As part of our ongoing studies into nucleophilic fluorination under hydrogen bonding phase-transfer catalysis (HBPTC),⁵ the issue of regiocontrolled fluorination arose. In 2019, we reported the enantioselective desymmetrization of *meso*-aziridinium ions with alkali metal fluoride using BINAM-derived *N*-alkylated *bis*-urea catalysts (Scheme 1A).^{5d} The resulting β -fluoroamines are formed in high yields and enantiomeric excesses. In this process, the insoluble fluoride salt is solubilized in the presence of a chiral HBD *bis*-urea phase transfer catalyst. The resulting hydrogen-bonded fluoride is a competent nucleophile in the enantiocontrolled reaction with the cationic electrophilic aziridinium partner via the formation of a chiral ion pair. Building on these precedents, hydrogen bonding catalysis applied to the regiocontrolled fluorination of dissymmetric aziridinium salts would represent a significant advance, with the prospect of offering new opportunities in regiodivergent asymmetric organocatalysis. The most attractive scenario

would employ a chiral hydrogen-bond donor catalyst to accelerate the fluorination of both enantiomers of a racemic mixture along regiodivergent pathways.

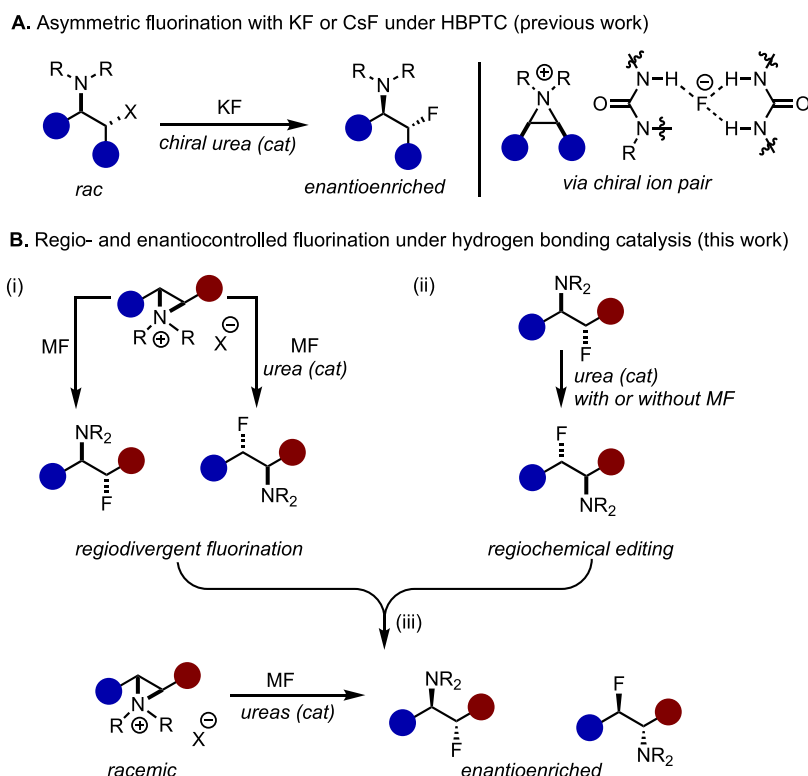
We noted two examples of regiodivergent parallel kinetic resolutions of aziridines with nitrogen and carbon nucleophiles carried out under transition-metal catalysis. In 2009, Parquette and RajanBabu reported that a dimeric yttrium-salen complex can induce divergent regioselectivities in the ring-opening reaction of racemic terminal aziridines with trimethylsilylazide.⁶ More recently, Shibasaki and Matsunaga broadened the synthetic utility of the process to internal aziridines and nucleophilic malonates applying combined Lewis acid [Y(OTf)₃] and Brønsted base [La(OiPr)₃] catalysis.⁷ To date, no solution is available to program the regiochemical outcome of the ring opening of dissymmetric aziridinium salts using an inexpensive alkali metal fluoride as the fluorinating reagent.

Herein, we report new approaches for regiocontrolled fluorination using HBD catalysis.⁸ First, we demonstrate that the kinetic regiopreference in the fluorination of dissymmetric β -chloroamines with an alkali metal fluoride can be inverted in the presence of a hydrogen bonding urea catalyst that attenuates the

Received: February 5, 2023

Published: April 20, 2023



Scheme 1. Regiocontrolled Ring Opening of Aziridinium ions with Alkali Metal Fluoride^a

^a(A) Enantioselective fluorination of *meso*-aziridinium salts with KF under HBPTC; (B) this work: (i) kinetic regiodivergence in nucleophilic substitution with alkali metal fluoride under hydrogen bonding catalysis, (ii) thermodynamic regiochemical editing under hydrogen bonding catalysis, and (iii) regiodivergent kinetic resolution of dissymmetric aziridinium ions with alkali metal fluoride.

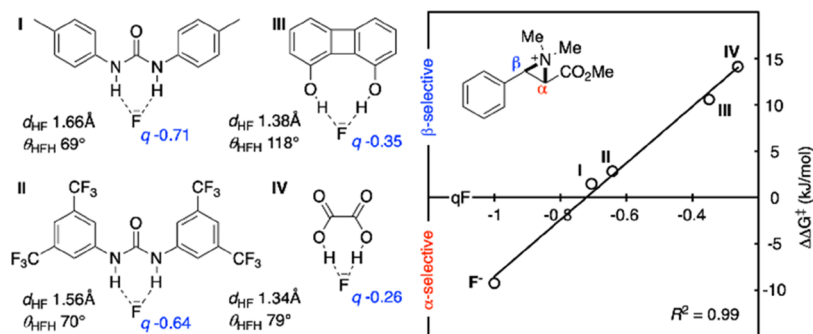


Figure 1. Computed levels of regioselectivity in nucleophilic fluorination with and without hydrogen-bond donor coordination (ω B97X-D3/(ma)-def2-TZVPP)//M06-2X/def2-SVP(TZVPPD).¹³ Löwdin charges q_F are shown.

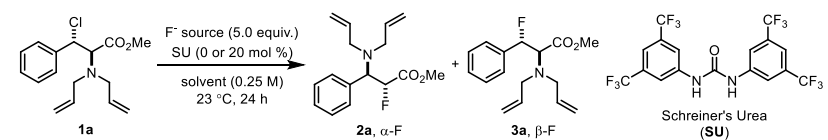
charge of fluoride (Scheme 1B, (i)). Second, the regiochemical editing of vicinal fluoroamines, consisting of C–F bond scission followed by fluoride rebound under hydrogen bonding catalysis, is unveiled (Scheme 1B, (ii)). Third, we disclose a protocol to access enantioenriched regioisomeric α - and β -fluoroamines using KF, a chiral BINAM-derived *bis*-urea catalyst, and the Schreiner's urea catalyst (Scheme 1B, (iii)).

RESULTS AND DISCUSSION

Regiocontrolled Ring Opening of *rac*-Aziridinium Ions with Alkali Metal Fluoride with and without Hydrogen-Bond Donor Catalyst: A Computational and Experimental Analysis. Sharpless and co-workers reported that the regiochemical preference for the ring opening of aziridinium salts with phenyl and ester substitution depends on the

nucleophile.⁹ Thiolate nucleophiles react α to the carboxylic ester, while opening at the benzylic position was preferred for amine nucleophiles. Controlling access to one or the other regioisomer upon opening of a dissymmetric aziridinium salt with an alkali metal fluoride nucleophile is, therefore, not a trivial problem.¹⁰ We envisioned that attenuation of the charge density of fluoride through hydrogen bonding may be a viable approach to reroute nucleophilic substitution toward the otherwise disfavored regioisomer. Preliminary computational studies were performed to explore this hypothesis. We considered the addition of a fluoride nucleophile to a dissymmetric aziridinium ion with phenyl and methyl ester substituents (Figure 1).

Quantum chemical calculations were used to compute the regioisomeric transition structures (TSs) and to predict the regioselectivity ($\Delta\Delta G^\ddagger$) for a free fluoride anion and fluoride

Table 1. Regiodivergence in Nucleophilic Fluorination of 1a with and without Schreiner's Urea Catalyst^a


entry	fluoride source	solvent	SU (mol %)	yield ^b	r.r. ^c 2a:3a
1	CsF	DCM	0	34%	>20:1
2	CsF	DCM	20	>95%	1:2.6
3	KF	DCM	0	0%	
4	KF	DCM	20	>95%	1:2.8
5	CsF	1,2-DFB	0	4%	α only
6	CsF	1,2-DFB	20	70%	1:2.4
7	KF	1,2-DFB	0	0%	
8	KF	1,2-DFB	20	>95%	1:4
9	NEt ₃ ·3HF	DCM	0	<10%	1:15
10	TBAF ^d	DCM	0	20%	1.3:1

^aReaction conditions: 0.1 mmol of **1a**, SU (0 or 20 mol %), and KF, CsF, or NEt₃·3HF (5.0 equiv) were stirred in dichloromethane (0.25 M) at 1200 rpm for 24 h. ^bDetermined by ¹H NMR using 1,3,5-trimethoxybenzene as an internal standard. ^cr.r. = regioisomeric ratio, determined by ¹H NMR of crude mixture. ^d6.0 equiv tetrabutylammonium fluoride. SU = Schreiner's urea.

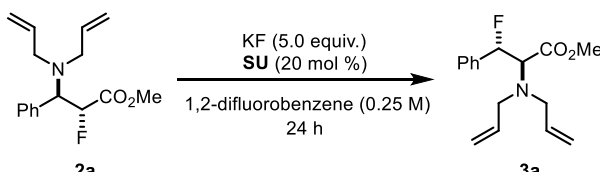
bound to four bidentate HBD moieties.^{11,12} The predicted regioselectivity is highly dependent upon the strength of coordination to the fluoride anion: while a free fluoride favors addition to the α -position by 9 kJ/mol, coordination to oxalic acid (IV) results in a preference for the β -position by 14 kJ/mol. Indeed, upon collecting structural and electronic parameters for the fluoride species I–IV, we obtained a linear correlation between $\Delta\Delta G^\ddagger$ for nucleophilic attack and the charge on F. As the HBD acidity increases, more negative charge is transferred from F in the complex and tighter complexes (with shorter H–F distances) are formed. These studies indicate that the electronic environment on fluoride, and hence control over regioselectivity in nucleophilic fluorination, can be rationally tuned through bidentate coordination with HBD catalysts.

We then turned to the experimental validation of this hypothesis with dissymmetric nonterminal aziridinium chlorides. The ring opening of *rac*-aziridinium chloride derived from the model *rac*-2-amino-3-chloro-3-aryl propanoic ester **1a** served to investigate the ability of 1,3-bis[3,5-bis(trifluoromethyl)phenyl]urea (SU, Schreiner's urea) to influence regioselectivity.

Fluorination with CsF in DCM at ambient temperature afforded preferentially β -amino- α -fluoroester **2a** (r.r. > 20:1, α : β) (Table 1, entry 1). The low conversion of 34% was expected as the reaction was carried out in the absence of an exogenous phase transfer agent for CsF solubilization. In the presence of 20 mol % of SU under otherwise identical conditions, fluorination is quantitative due to the ability of the SU catalyst to bring CsF into solution. Significantly, the kinetic regiopreference of fluoride is reversed, now favoring the formation of the β -fluoro- α -aminoester **3a** (r.r. = 1:2.6, α : β) (Table 1, entry 2). The urea-catalyzed reaction also led predominantly to **3a** with KF (r.r. = 1:2.8, α : β), a fluoride source that does not react in the absence of SU catalyst (Table 1, entries 3 and 4). Similar trends were obtained in 1,2-difluorobenzene, a solvent of choice for fluorination reactions carried out under HBPTC⁶ (Table 1, entries 5–8). The soluble fluoride source NEt₃·3HF displayed preferential β -fluorination, but **2a** and **3a** were formed in low yields due to the decomposition of the starting material (Table 1, entry 9). A poor yield was also observed with TBAF, a reagent displaying

overall poor regiocontrol (Table 1, entry 10). Slow release of soluble fluoride, which is achieved with alkali metal fluoride brought into solution by the urea phase transfer catalyst, enhances conversion to the desired fluorinated products.

Considering that hydrogen-bond donors are capable of C–F bond polarization,¹⁴ the possibility of reversible fluorination was probed experimentally. These experiments were carried out in 1,2-difluorobenzene (b.p. 94 °C). We subjected the α -fluorinated product **2a** to the reaction conditions at increasing temperatures. After 24 h at room temperature, the β -regioisomer was detectable (Table 2, entry 1), and as the temperature

Table 2. Regiochemical Editing through a Urea-Catalyzed Defluorination-Fluorination Pathway^a


entry	T (°C)	yield ^b (2a + 3a)	r.r. ^c (2a : 3a)
1	23	>95%	13.4:1
2	40	>95%	2.9:1
3	60	>95%	1:20
4 ^d	60	>95%	α only
5 ^e	60	59%	1:6.8

^aReaction conditions: 0.1 mmol of **2a**, SU (20 mol %), and KF (5 equiv) were stirred in 1,2-difluorobenzene at 1200 rpm for 24 h.

^bDetermined by ¹H NMR using 1,3,5-trimethoxybenzene as an internal standard. ^cr.r. = regioisomeric ratio, determined by ¹H NMR of crude mixture. ^dReaction performed without Schreiner's urea (SU).

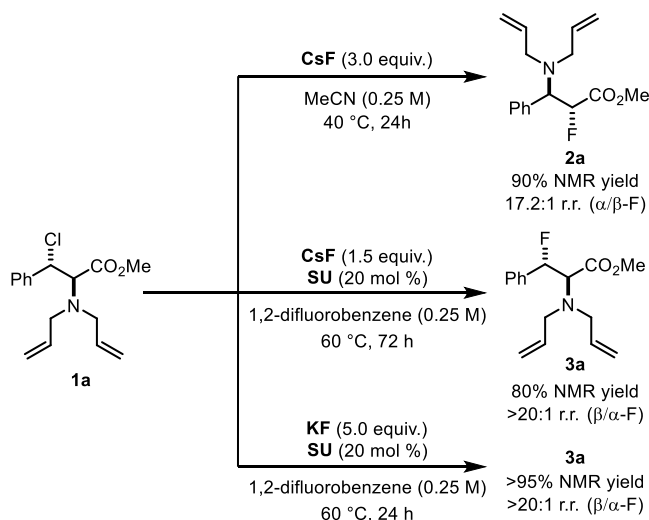
^eReaction performed without KF. SU = Schreiner's urea.

increased, the defluorination-fluorination pathway became more efficient (Table 2, entries 2–3).¹⁵ A control experiment demonstrated that the α -regioisomer **2a** is fully recovered in the absence of Schreiner's urea catalyst at 60 °C (Table 2, entry 4). Moreover, β -**3a** was formed in 59% yield in the absence of KF under hydrogen bonding catalysis, a unique example of regiochemical editing through organocatalytic C–F bond scission and fluoride rebound (Table 2, entry 5).¹⁶ The

conversion of **2a** to **3a** constitutes a formal organocatalyzed dyotropic rearrangement with no erosion of stereochemistry observed upon fluoride transfer.

With these data in hand, further optimization varying the temperature, solvent, and reaction time provided reaction conditions to access the regioisomeric α - and β -fluoroamines **2a** and **3a** from **1a** in high regioselectivity and high yield from CsF. The β -fluoroamine **3a** was also within reach with KF under HBPTC with catalytic Schreiner's urea (SU) (Scheme 2).¹⁷

Scheme 2. Regiodivergence in Nucleophilic Fluorination with Alkali Metal Fluoride^a



^aSU = Schreiner's urea.

Computational studies gave further insight (Figure 2). Data secured with *N*-allyl modeled by *N*-methyl groups indicated that the α -position, whose attack is favored in the absence of urea, is characterized by a more positive electrostatic potential (Figure 2A). In contrast, at the β -position, which is the preferred site of attack with catalytic SU, there is greater contribution of the antibonding σ_{C-N}^* orbital to the LUMO (the LUMO + 1 has contribution from the σ_{C-N}^* to the α -position). LUMO and LUMO + 1 energies are very similar, rendering the application of FMO theory to understand regioselectivity challenging. The TS geometries for free fluoride are relatively early, with longer C–F/shorter C–N distances compared to the fluoride:HBD complex (Figure 2B). Greater electrostatic attraction at the α -carbon steers the regiochemical preference for this position. With fluoride bound to the SU catalyst, its negative charge and nucleophilicity are attenuated, leading to later TS geometries with shorter C–F/longer C–N distances (Figure 2C). Electrostatic interactions are less significant, and substrate distortion energies become more critical (vide infra). The β -fluoroamine is favored thermodynamically by 8.5 kJ/mol over the α -regioisomer. The potential energy surface (PES) for SU-catalyzed conversion of **2a** into **3a** was also studied computationally (Figure 3). At higher temperatures, **3a** is the major regioisomer formed, which is expected as it is thermodynamically more stable than **2a**. The fluorination TS leading to this product is also more favorable than that leading to the α -regioisomer by 3.1 kJ/mol, consistent with kinetically controlled regioselectivity for the β -regioisomer in the presence of SU catalyst.

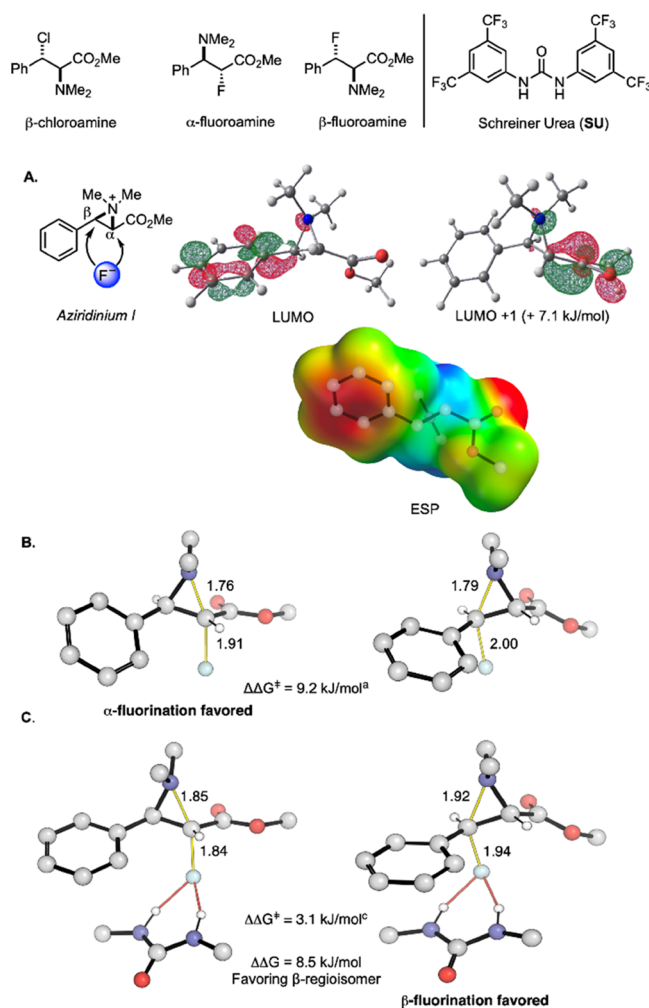


Figure 2. Computed ground and TS structures for aziridinium fluorination (B97X-D3/(ma)-def2-TZVPP//M06-2X/def2-SVP-(TZVPPD) with CPCM DCM solvation).¹³ (A) Aziridinium LUMO, LUMO + 1 and ESP plots. (B) TSs with free fluoride. (C) TSs with SU-bound fluoride (SU aryl rings abbreviated for clarity).

To gain further quantitative insight into the origins of the switch in regioselectivity in the presence of the Schreiner's urea, a distortion-interaction activation-strain analysis was performed along the fluorination intrinsic reaction coordinate (IRC) with and without catalyst (Figure 4).¹⁸ The difference between breaking (C–N) and forming (C–F) bonds was used as the reduced reaction coordinate. Further decomposition of the interaction energies into Pauli repulsion, orbital (polarization and charge transfer), electrostatic, and dispersion interactions was performed using the absolutely localized molecular orbital-energy decomposition analysis (ALMO-EDA).¹⁹ Selectivity in the uncatalyzed fluorination reaction is dictated by the difference in interaction energies (green curves). The approach of free fluoride at the α -position has a more favorable interaction energy by 23.2 kJ/mol, the result of a large stabilizing electrostatic attraction between nucleophile and electrophile for the attack at this position. This is consistent with the ESP map (Figure 2A), showing a more positive value around the α -carbon. Since the TS geometries are relatively early, substrate distortion terms are small. Overall, these results are consistent with electrostatically controlled selectivity with free fluoride. In contrast, when fluoride is bound to urea, distortion energy terms

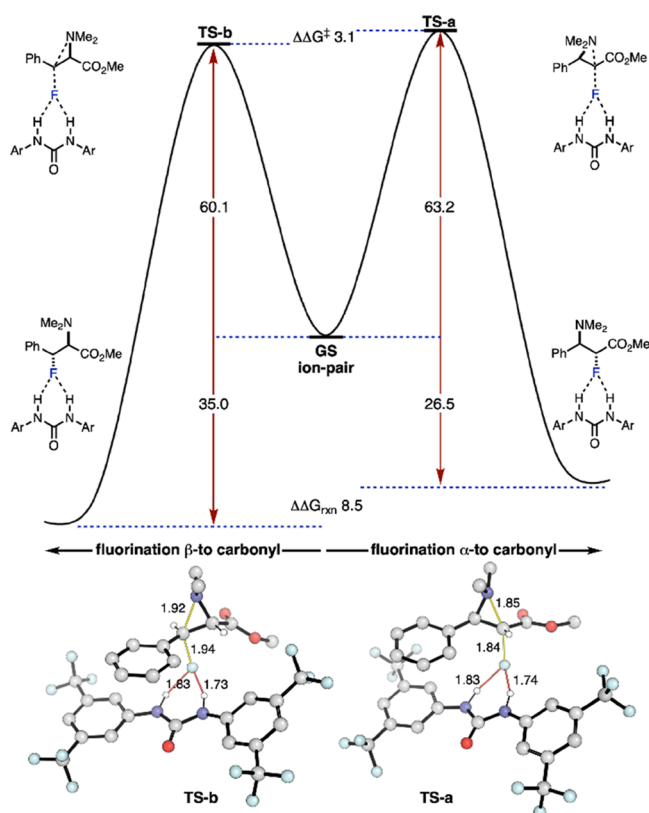


Figure 3. Computed PES for defluorination/fluorination sequence enabling the regiochemical editing of fluoroamines. (ω B97X-D3/(ma)-def2-TZVPP)//M06-2X/def2-SVP(TZVPPD).¹³ Ar = 3,5-bis-(trifluoromethyl)phenyl.

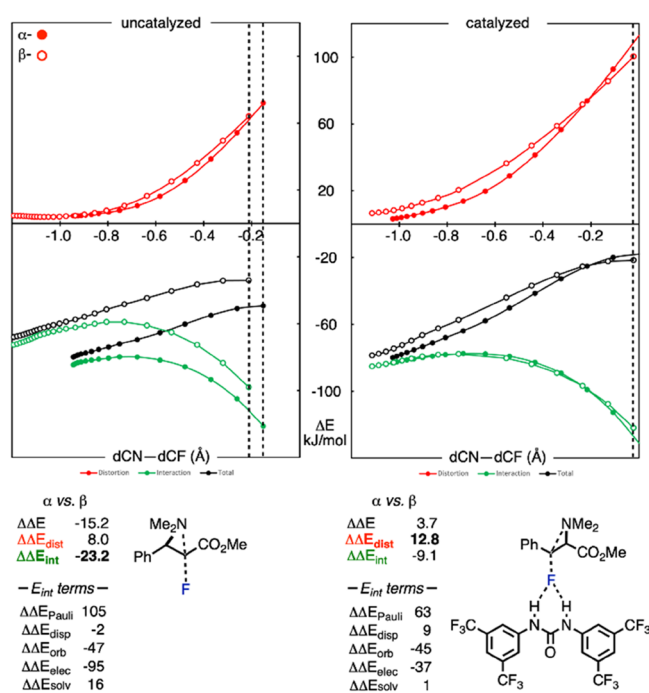


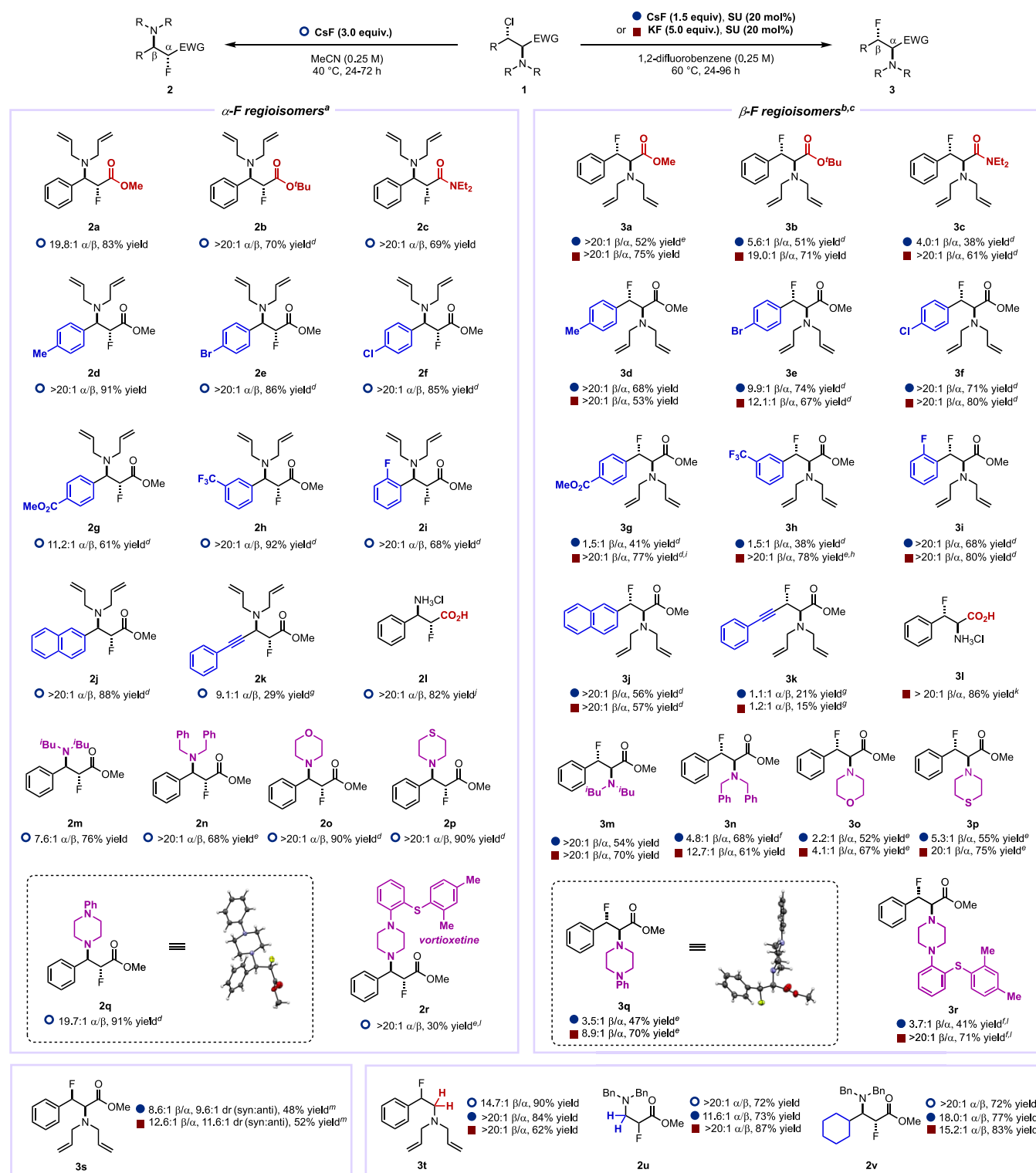
Figure 4. Distortion-interaction activation-strain analysis for aziridinium fluorination with and without Schreiner's urea (ω B97X-D3/def2-TZVPP with CPCM solvation).¹³ Filled circles = α -pathway; empty circles = β -pathway. TS positions are shown with dashed lines.

become more important: the TS is later, and so substrate distortion is larger. Interestingly, the distortion energy of the α -TS grows more sharply than the β -TS as the TS is approached; we ascribe this to the destabilizing accumulation of positive charge in the substrate α - to an electron-withdrawing ester group. At the same time, the electrostatic preference for the α -position is reduced (from 95 to 37 kJ/mol), presumably since F now bears less negative charge (-0.64 , Figure 1) compared to unbound fluoride. As a result, the difference in distortion energies dictates the regioselectivity. This term is mainly derived from the aziridinium electrophile, where lengthening of the β -C–N bond is less costly than the α -C–N bond, presumably due to the ability of the adjacent phenyl group to stabilize the developing positive charge in the distorted geometry.

Generalization and Asymmetric Regiodivergent Fluorination with an (S)-BINAM-Derived Urea Catalyst. With the optimized experimental protocols in hand, we sought to evaluate the scope of the regiodivergent fluorination reaction without and with SU catalyst (Scheme 3).²⁰

β -Chloroamines bearing various aryl, amino, ester, and amide substituents were first subjected to α -fluorination with CsF in MeCN at 40 °C. The reaction tolerates *tert*-butyl ester instead of methyl ester, providing **2b**, which was transformed into the α -fluoro- β -amino acid **2l**. Most aryl groups investigated afforded the α -regioisomers in a high α : β ratio ($>20:1$), but we noted that the regiopreference observed with **1g** featuring the electron-withdrawing methyl ester group at the para position was less pronounced (r.r. = 11.2:1, α : β). The aryl group can be replaced by propargyl albeit affording **2k** in lower yield and α : β ratio (9.1:1). Gratifyingly, the reaction is compatible with several amino groups including motifs frequently seen in medicinal chemistry such as, for example, piperidine and (thio)-morpholines. Next, we subjected the same library of β -chloroamines to β -fluorination using either KF or CsF in the presence of the Schreiner's urea (SU) catalyst. Higher β : α ratios were obtained with KF compared to CsF. This result was expected due to the lack of background reactivity of KF in the absence of SU catalyst under otherwise similar reaction conditions. Higher yields of isolated products were also often obtained with KF versus CsF. The reaction tolerates all substrates **1a–r** but underperformed for the propargylic fluoride **3k**, which was obtained as a mixture of regioisomers. When the electron-withdrawing ability of the aromatic substituent was increased, a higher temperature was required to achieve high regioselectivity (for **3g**, for instance). This catalytic reaction gives high regioselectivity with mildly electron-donating (**3d**) and halogen (**3e–3f**) substituents, although a longer reaction time was also required in the latter cases. Tertiary amines, including the bulkier diisobutylamine (**3m**), saturated heterocycles (**3o–3q**), and a biologically active motif (**3r**), were well tolerated. The *cis*-aziridinium precursor gave **3s** in good regioselectivity (r.r. = 12.6:1, β : α) along with a detectable amount of the *anti*-diastereomer. A substrate lacking the ester motif resulted in regioselective benzylic fluorination (**3t**) under all reaction conditions. Conversely, when a serine-derived starting material lacking the aryl group was employed (**1u**), α -fluorination was invariably observed. A similar α -regiopreference was observed with a cyclohexyl substituent (**3v**). This change in regioselectivity is consistent with the LUMO coefficient localized on the carbon α to the ester for these substrates.¹⁷

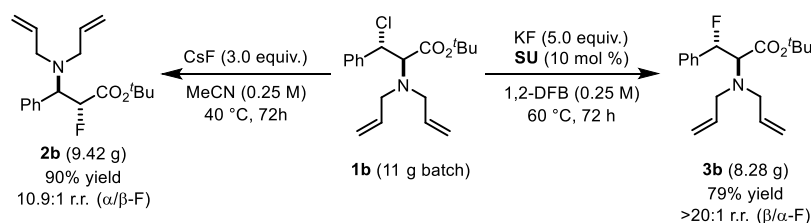
Multigram quantities of both regioisomers **2b** and **3b** were obtained from β -chloroamine **1b** (Scheme 4). Starting with 11 g

Scheme 3. Scope of α - and β -Fluorination of β -Chloroamines^{a,b,c,d,e,f,g,h,i,j,k,l}

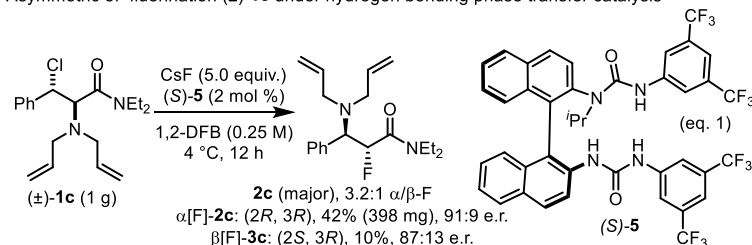
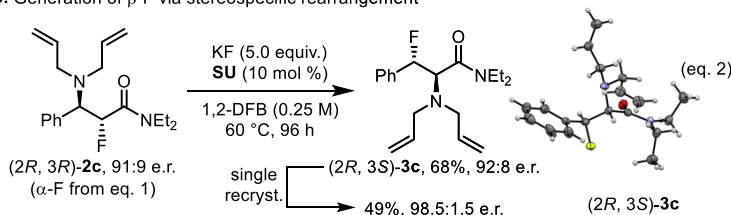
^aReaction conditions for α -F regioisomers: 0.25 mmol of β -chloroamine and CsF (3.0 equiv) were stirred in MeCN (1.0 mL, 0.25 M) at 1200 rpm for 24 h at 40 °C. ^bReaction conditions for β -F regioisomers: (b) 0.25 mmol of β -chloroamine, SU (20 mol %), and KF (5.0 equiv) or (c) 0.25 mmol of β -chloroamine, SU (20 mol %), and CsF (1.5 equiv) were stirred in 1,2-DFB (1.0 mL, 0.25 M) at 1200 rpm for 24 h at 60 °C. ^cReaction was run for 48 h. ^dReaction was run for 72 h. ^eReaction was run for 96 h. ^fReaction at 23 °C. ^gReaction at 70 °C. ^hReaction at 80 °C. ⁱObtained from 2b. ^jObtained from 3b. ^kReaction at 0.15 mmol scale. ^lYield determined by quantitative ¹H NMR, using 1,3,5-trimethoxybenzene as an internal standard.

of 1b, 8.28 g of β -fluoroamine 3b (r.r. > 20:1) was isolated when the reaction was performed with KF (5 equiv) and SU catalyst

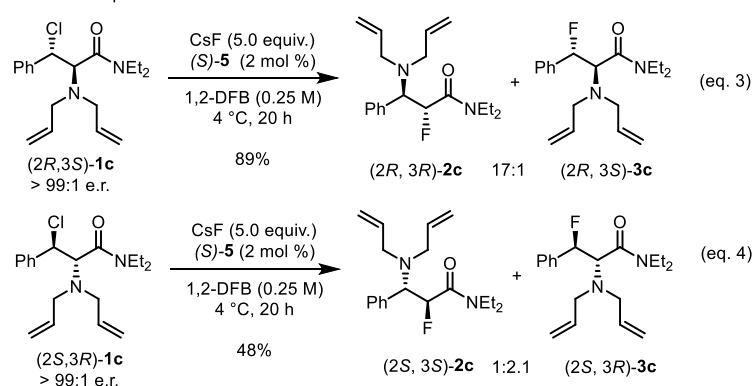
(10 mol %) at 60 °C. A reaction time of 72 h was necessary to reach 79% yield. The fluorination of 11 g of 1b with CsF (3

Scheme 4. Multigram Synthesis of **2b** and **3b**

Scheme 5. Regiocontrolled Fluorination under Asymmetric Hydrogen Bonding Phase Transfer Catalysis

A. Asymmetric α -fluorination (\pm)-**1c** under hydrogen bonding phase transfer catalysisB. Generation of β -F via stereospecific rearrangement

C. Control experiments



equiv) in MeCN at 40 °C for 72 h afforded 9.42 g of α -fluoroamine **2b** (r.r. > 10:1).

Having demonstrated regiodivergence under hydrogen bonding catalysis, we considered the BINAM-derived (*S*)-bis-urea catalyst **5** to prepare enantioenriched fluoroamines. Early experimentations identified the β -chloro- α -amino amide (\pm)-**1c** as a promising substrate for this study.¹⁷ The reaction of (\pm)-**1c** with CsF in 1,2-difluorobenzene at 4 °C in the presence of 2 mol % of (*S*)-**5** gave α [F]-**2c** as the preferential regioisomer (r.r. = 3.2:1, α/β) in enantioenriched form (91:9 e.r.). The minor regioisomer was also formed with significant enantioenrichment (87:13 e.r.). (Scheme 5, eq 1). Furthermore, when enantioenriched α [F]-**2c** was subjected to stereospecific fluoride migration in the presence of KF and the Schreiner's urea (Scheme 5, eq 2), the β -fluorinated product β [F]-**3c** was formed with no erosion of enantiomeric ratio; to proceed, this rearrangement required elevated temperature (60 °C). Control experiments with enantiopure (*2R*,3*S*)-**1c** and (*2S*,3*R*)-**1c** gave useful insight.²¹ The reaction of (*2R*,3*S*)-**1c** (>99:1 e.r.) with

CsF in the presence of 2 mol % of the BINAM-derived (*S*)-bis-urea catalyst **5** led to regioisomers **2c** and **3c** with **2c** being largely predominant (r.r. = 17:1, α/β) (Scheme 5, eq 3). Enantiomer (*2R*,3*S*)-**1c** under the same reaction conditions was consumed less rapidly and led to two regioisomers with a ratio now favoring β -fluorination (r.r. = 1:2.1, α/β) (Scheme 5, eq 4). These results indicate that the regiopreference of the catalyst allows divergent reaction pathways for each enantiomer with fluorination proceeding with unequal rates. The exact origin of the regiopreference of this catalyst remains to be established. It is conceivable that the chiral urea–fluoride complex binds the two enantiomers of the aziridinium ion in distinct orientations during the activation process, and each of the diastereomeric complexes has a different electrophilic carbon favorably exposed for attack by fluoride.

CONCLUSIONS

This work has unveiled a novel approach to invert the sense of regiocontrol for fluorination with alkali metal fluoride through a modulation of charge density on fluoride with a hydrogen-bond donor phase transfer catalyst. Combined with a novel HBD-enabled regiochemical editing process consisting of an equilibration mechanism based on urea-catalyzed C–F activation followed by fluoride rebound, high regioisomeric ratios in favor of either regioisomer are within reach using an alkali metal fluoride as fluorination reagent. Moreover, the synthesis of regio- and enantioenriched α - and β -fluoroamines under asymmetric hydrogen bonding catalysis with a BINAM-derived bis-urea catalyst offers new opportunities to expand the scope of synthetic strategies available to access fluorinated molecules. More generally, this catalyst-controlled approach to alter regiochemical preference may be applicable to many electrophiles and charged nucleophiles other than alkali metal fluoride.

ASSOCIATED CONTENT

Supporting Information

The Supporting Information is available free of charge at <https://pubs.acs.org/doi/10.1021/jacs.3c01303>.

Experimental details, characterization data, NMR spectra, and full computational details (PDF)

Computational data_xyz_coordinates (ZIP)

Computational data_MP2_alpha_TS.xyz (XYZ)

Computational data_MP2_beta_TS.xyz (XYZ)

Accession Codes

CCDC 2232281–2232283 contain the supplementary crystallographic data for this paper. These data can be obtained free of charge via www.ccdc.cam.ac.uk/data_request/cif, or by emailing data_request@ccdc.cam.ac.uk, or by contacting The Cambridge Crystallographic Data Centre, 12 Union Road, Cambridge CB2 1EZ, UK; fax: +44 1223 336033.

AUTHOR INFORMATION

Corresponding Authors

Matthew A. Horwitz – Chemistry Research Laboratory, University of Oxford, Oxford OX1 3TA, U.K.; Email: mah9122@gmail.com

Alexander B. Dürr – Chemistry Research Laboratory, University of Oxford, Oxford OX1 3TA, U.K.; Email: alexanderbdurr.chemistry@gmail.com

Robert S. Paton – Department of Chemistry, Colorado State University, Fort Collins, Colorado 80528, United States; orcid.org/0000-0002-0104-4166; Email: robert.paton@colostate.edu

Véronique Gouverneur – Chemistry Research Laboratory, University of Oxford, Oxford OX1 3TA, U.K.; orcid.org/0000-0001-8638-5308; Email: veronique.gouverneur@chem.ox.ac.uk

Authors

Konstantinos Afratis – Chemistry Research Laboratory, University of Oxford, Oxford OX1 3TA, U.K.

Zijun Chen – Chemistry Research Laboratory, University of Oxford, Oxford OX1 3TA, U.K.

Julia Soika – Chemistry Research Laboratory, University of Oxford, Oxford OX1 3TA, U.K.

Kirsten E. Christensen – Chemistry Research Laboratory, University of Oxford, Oxford OX1 3TA, U.K.

Makoto Fushimi – Takeda Pharmaceutical Company Limited, Fujisawa, Kanagawa 251-8555, Japan

Complete contact information is available at: <https://pubs.acs.org/doi/10.1021/jacs.3c01303>

Author Contributions

[†]M.A.H., A.B.D., K.A., and Z.C. contributed equally to this work.

Notes

The authors declare no competing financial interest.

ACKNOWLEDGMENTS

This work was supported by Merton College (Chemistry Scholarship to K.A.), the EU Horizon 2020 Research and Innovation Programme (Marie Skłodowska-Curie Agreement 890535), the Engineering and Physical Sciences Research Council (EP/R010064), the European Research Council (Agreement 832994), the Alfred Krupp von Bohlen and Halbach Foundation (J.S.), and Takeda Pharmaceutical Company Limited (COCKPI-T Funding Programme). R.S.P. acknowledges support from the National Science Foundation (CHE 1955876) and the Extreme Science and Engineering Discovery Environment (XSEDE) through allocation TG-CHE180056. The authors gratefully acknowledge the EPSRC for the provision of a single-crystal X-ray diffractometer under the Strategic Equipment Grant EP/V028995/1. Calum Patel is gratefully acknowledged for assistance with X-ray crystallography.

REFERENCES

- (1) (a) Xiang, S. H.; Tan, B. *Advances in Asymmetric Organocatalysis over the Last 10 Years*. *Nat. Commun.* **2020**, *11*, No. 3786. (b) Han, B.; He, X. H.; Liu, Y. Q.; He, G.; Peng, C.; Li, J. L. *Asymmetric Organocatalysis: An Enabling Technology for Medicinal Chemistry*. *Chem. Soc. Rev.* **2021**, *50*, 1522–1586.
- (2) (a) Zhan, G.; Du, W.; Chen, Y.-C. Switchable Divergent Asymmetric Synthesis via Organocatalysis. *Chem. Soc. Rev.* **2017**, *46*, 1675–1692. (b) Viji, M.; Lanka, S.; Sim, J.; Jung, C.; Lee, H.; Vishwanath, M.; Jung, J.-K. Regiodivergent Organocatalytic Reactions. *Catalysts* **2021**, *11*, 1013.
- (3) Dale, H. J. A.; Hodges, G. R.; Lloyd-Jones, G. C. Taming Ambident Triazole Anions: Regioselective Ion Pairing Catalyzes Direct N-Alkylation with Atypical Regioselectivity. *J. Am. Chem. Soc.* **2019**, *141*, 7181–7193.
- (4) (a) Guo, C.; Fleige, M.; Janssen-Müller, D.; Daniliuc, C. G.; Glorius, F. Switchable Selectivity in an NHC-Catalysed Dearomatizing Annulation Reaction. *Nat. Chem.* **2015**, *7*, 842–847. (b) Guo, C.; Sahoo, B.; Daniliuc, C. G.; Glorius, F. N-Heterocyclic Carbene Catalyzed Switchable Reactions of Enals with Azoalkenes: Formal [4 + 3] and [4 + 1] Annulations for the Synthesis of 1,2-Diazepines and Pyrazoles. *J. Am. Chem. Soc.* **2014**, *136*, 17402–17405.
- (5) (a) Engle, K. M.; Pfeifer, K.; Pidgeon, G. W.; Giuffredi, G. T.; Thompson, A. L.; Paton, R. S.; Brown, J. M.; Gouverneur, V. Coordination Diversity in Hydrogen-Bonded Homoleptic Fluoride–Alcohol Complexes Modulates Reactivity. *Chem. Sci.* **2015**, *6*, 5293–5302. (b) Pfeifer, L.; Engle, K. M.; Pidgeon, G. W.; Sparkes, H. A.; Thompson, A. L.; Brown, J. M.; Gouverneur, V. Hydrogen-Bonded Homoleptic Fluoride–Diaryliurea Complexes: Structure, Reactivity, and Coordinating Power. *J. Am. Chem. Soc.* **2016**, *138*, 13314–13325. (c) Pupo, G.; Ibba, F.; Ascough, D. M. H.; Vicini, A. C.; Ricci, P.; Christensen, K. F.; Pfeifer, L.; Morphy, J. R.; Brown, J. M.; Paton, R. S.; Gouverneur, V. Asymmetric Nucleophilic Fluorination under Hydrogen Bonding Phase-Transfer Catalysis. *Science* **2018**, *360*, 638–642. (d) Pupo, G.; Vicini, A. C.; Ascough, D. M. H.; Ibba, F.; Christensen, K. E.; Thompson, A. L.; Brown, J. M.; Paton, R. S.; Gouverneur, V. Hydrogen Bonding Phase-Transfer Catalysis with Potassium Fluoride:

- Enantioselective Synthesis of β -Fluoroamines. *J. Am. Chem. Soc.* **2019**, *141*, 2878–2883. (e) Roagna, G.; Ascough, D. M. H.; Ibba, F.; Vicini, A. C.; Fontana, A.; Christensen, K. E.; Peschiulli, A.; Oehrich, D.; Misale, A.; Trabanco, A. A.; Paton, R. S.; Pupo, G.; Gouverneur, V. Hydrogen Bonding Phase-Transfer Catalysis with Ionic Reactants: Enantioselective Synthesis of γ -Fluoroamines. *J. Am. Chem. Soc.* **2020**, *142*, 14045–14051. (f) Vicini, A. C.; Alozie, D.-M.; Courtes, P.; Roagna, G.; Aubert, C.; Certal, V.; El-Ahmad, Y.; Roy, S.; Gouverneur, V. Scalable Synthesis of (R,R)-N,N-Dibenzyl-2-fluorocyclohexan-1-amine with CsF under Hydrogen Bonding Phase-Transfer Catalysis. *Org. Process Res. Dev.* **2021**, *25*, 2730–2737.
- (6) Wu, B.; Gallucci, J.; Parquette, J.; RajanBabu, T. Enantioselective Desymmetrization of *meso*-Aziridines with TMSN₃ or TMSCN Catalyzed by Discrete Yttrium Complexes. *Angew. Chem., Int. Ed.* **2009**, *48*, 1126–1129.
- (7) Xu, Y.; Lin, L.; Kanai, M.; Matsunaga, S.; Shibasaki, M. Catalytic Asymmetric Ring-Opening of *meso*-Aziridines with Malonates under Heterodinuclear Rare Earth Metal Schiff Base Catalysis. *J. Am. Chem. Soc.* **2011**, *133*, 5791–5793.
- (8) Katcher, M. H.; Sha, A.; Doyle, A. G. Palladium-Catalyzed Regio- and Enantioselective Fluorination of Acyclic Allylic Halides. *J. Am. Chem. Soc.* **2011**, *133*, 15902–15905.
- (9) (a) Chuang, T. H.; Sharpless, K. B. Applications of Aziridinium Ions. Selective Syntheses of β -Aryl- α,β -diamino Esters. *Org. Lett.* **1999**, *1*, 1435–1437. (b) Chuang, T. H.; Sharpless, K. B. Applications of Aziridinium Ions. Selective Syntheses of α,β -Diamino Esters, α -Sulfanyl- β -amino Esters, β -Lactams, and 1,5-Benzodiazepin-2-one. *Org. Lett.* **2000**, *2*, 3555–3557.
- (10) Selected studies employing fluorinating reagents other than alkali metal fluoride for the ring opening of a dissymmetric aziridinium salt: (a) Morlot, M.; Gourand, F.; Perrio, C. Deoxyradiofluorination Reaction from β -Hydroxy- α -aminoesters: an Entry to [¹⁸F]-Fluoroaminoesters under Mild Conditions. *Eur. J. Org. Chem.* **2019**, *2019*, 3751–3762. (b) Davies, S. G.; Fletcher, A. M.; Frost, A. B.; Roberts, P. M.; Thomson, J. E. Asymmetric Synthesis of Substituted *anti*- β -Fluorophenylalanines. *Org. Lett.* **2015**, *17*, 2254–2257. (c) Zhu, L.; Xiong, J.; An, J.; Chen, N.; Xue, J.; Jiang, X. Highly Efficient Regio-Selective Ring-Opening Nucleophilic Fluorination of Aziridines and Azetidines: Access to β - or γ -Fluorinated Amino Acid Derivatives. *Biomol. Chem.* **2019**, *17*, 3797–3804. (d) Adler, P.; Teskey, C. J.; Kaiser, D.; Holy, M.; Sitte, H. H.; Maulide, N. α -Fluorination of Carbonyls with Nucleophilic Fluorine. *Nat. Chem.* **2019**, *11*, 329–334.
- (11) (a) Klopman, G. Chemical Reactivity and the Concept of Charge- and Frontier-Controlled Reactions. *J. Am. Chem. Soc.* **1968**, *90*, 223–234. (b) Salem, L. Intermolecular Orbital Theory of the Interaction Between Conjugated Systems. I. General Theory. *J. Am. Chem. Soc.* **1968**, *90*, 543–552.
- (12) Zhuo, L. G.; Liao, W.; Yu, Z. X. A Frontier Molecular Orbital Theory Approach to Understanding the Mayr Equation and to Quantifying Nucleophilicity and Electrophilicity by Using HOMO and LUMO Energies. *Asian J. Org. Chem.* **2012**, *1*, 336–345.
- (13) (a) Zhao, Y.; Truhlar, D. G. The M06 Suite of Density Functionals for Main Group Thermochemistry, Thermochemical Kinetics, Noncovalent Interactions, Excited States, and Transition Elements: Two New Functionals and Systematic Testing of Four M06-Class Functionals and 12 Other Functionals. *Theor. Chem. Acc.* **2008**, *120*, 215–241. (b) Frisch, M. J.; Trucks, G. W.; Schlegel, H. B.; Scuseria, G. E.; Robb, M. A.; Cheeseman, J. R.; Scalmani, G.; Barone, V.; Mennucci, B.; Nakatsuji, G. A.; Caricato, M.; Li, X.; Hratchian, H. P.; Izmaylov, A. F.; Bloino, J.; Zheng, G.; Sonnenberg, J. L.; Hada, M.; Ehara, M.; Toyota, K.; Fukuda, R.; Hasegawa, J.; Ishida, M.; Nakajima, T.; Honda, Y.; Kitao, O.; Nakai, H.; Vreven, T.; Montgomery, J. A., Jr.; Peralta, J. E.; Ogliaro, F.; Bearpark, M.; Heyd, J. J.; Brothers, E.; Kudin, K. N.; Staroverov, V. N.; Kobayashi, R.; Normand, J.; Raghavachari, K.; Rendell, A.; Burant, J. C.; Iyengar, S. S.; Tomasi, J.; Cossi, M.; Rega, N.; Millam, J. M.; Klene, M.; Knox, J. E.; Cross, J. B.; Bakken, V.; Pomelli, C.; Ochterski, J. W.; Martin, R. L.; Morokuma, K.; Zakrzewski, V. G.; Voth, G. A.; Salvador, P.; Dannenberg, J. J.; Dapprich, S.; Daniels, A. D.; Farkas, Ö.; Foresman, J. B.; Ortiz, J. V.; Cioslowski, J.; Fox, D. J. *Gaussian 09*. Revision D.01; Gaussian, Inc: Wallingford CT, 2009.
- (c) Takano, Y.; Houk, K. N. Benchmarking the Conductor-like Polarizable Continuum Model (CPCM) for Aqueous Solvation Free Energies of Neutral and Ionic Organic Molecules. *J. Chem. Theory Comput.* **2005**, *1*, 70–77. (d) Cossi, M.; Rega, N.; Scalmani, G.; Barone, V. Energies, Structures, and Electronic Properties of Molecules in Solution with the C-PCM Solvation Model. *J. Comput. Chem.* **2003**, *24*, 669–681. (e) Barone, V.; Cossi, M. Quantum Calculation of Molecular Energies and Energy Gradients in Solution by a Conductor Solvent Model. *J. Phys. Chem. A* **1998**, *102*, 1995–2001. (f) Neese, F. The ORCA Program System. *Wiley Interdiscip. Rev. Comput. Mol. Sci.* **2012**, *2*, 73–78. (g) Neese, F. Software Update: the ORCA Program System, Version 4.0. *Wiley Interdiscip. Rev. Comput. Mol. Sci.* **2018**, *8*, No. e1327. (h) Chai, J. D.; Head-Gordon, M. Long-Range Corrected Hybrid Density Functionals with Damped Atom–Atom Dispersion Corrections. *Phys. Chem. Chem. Phys.* **2008**, *10*, 6615–6620. (i) Lin, Y. S.; Li, G. D.; Mao, S. P.; Chai, J. D. Long-Range Corrected Hybrid Density Functionals with Improved Dispersion Corrections. *J. Chem. Theory Comput.* **2013**, *9*, 263–272. (j) Grimme, S.; Antony, J.; Ehrlich, S.; Krieg, H. A Consistent and Accurate *ab initio* Parametrization of Density Functional Dispersion Correction (DFT-D) for the 94 Elements H–Pu. *J. Chem. Phys.* **2010**, *132*, No. 154104. (k) Zheng, J.; Xu, X.; Truhlar, D. G. Minimally Augmented Karlsruhe Basis Sets. *Theor. Chem. Acc.* **2011**, *128*, 295–305. (l) Weigend, F.; Ahlrichs, R. Balanced Basis Sets of Split Valence, Triple Zeta Valence and Quadruple Zeta Valence Quality for H to Rn: Design and Assessment of Accuracy. *Phys. Chem. Chem. Phys.* **2005**, *7*, 3297–3305. (m) Rappoport, D.; Furche, F. Property-Optimized Gaussian Basis Sets for Molecular Response Calculations. *J. Chem. Phys.* **2010**, *133*, No. 134105. (n) Hellweg, A.; Rappoport, D. Development of New Auxiliary Basis Functions of the Karlsruhe Segmented Contracted Basis Sets Including Diffuse Basis Functions (def2-SVPD, def2-TZVPPD, and def2-QVPPD) for RI-MP2 and RI-CC Calculations. *Phys. Chem. Chem. Phys.* **2015**, *17*, 1010–1017. (o) Luchini, G.; Alegre-Requena, J. V.; Funes-Ardoiz, I.; Paton, R. S. GoodVibes: Automated Thermochemistry for Heterogeneous Computational Chemistry Data. *FI1000Research* **2020**, *9*, 291. (p) Grimme, S. Supramolecular Binding Thermodynamics by Dispersion-Corrected Density Functional Theory. *Chem.–Eur. J.* **2012**, *18*, 9955–9964.
- (14) Houle, C.; Savoie, P. R.; Davies, C.; Jardel, D.; Champagne, P. A.; Bibal, B.; Paquin, J. F. Thiourea-Catalyzed C–F Bond Activation: Amination of Benzylic Fluorides. *Chem.–Eur. J.* **2020**, *26*, 10620–10625.
- (15) Métro, T.-X.; Duthion, B.; Pardo, D. G.; Cossy, J. Rearrangement of β -Amino Alcohols via Aziridiniums: A Review. *Chem. Soc. Rev.* **2010**, *39*, 89–102.
- (16) (a) Levin, M. D.; Chen, T. Q.; Neubig, M. E.; Hong, C. M.; Theulier, C. A.; Kobylanski, I. J.; Janabi, M.; O’Neil, J. P.; Toste, F. D. A Catalytic Fluoride-Rebound Mechanism for C(sp³)-CF₃ Bond Formation. *Science* **2017**, *356*, 1272–1276. (b) Fujimoto, H.; Kodama, T.; Yamanaka, M.; Tobisu, M. Phosphine-Catalyzed Intermolecular Acylfluorination of Alkynes via a P(V) Intermediate. *J. Am. Chem. Soc.* **2020**, *142*, 17323–17328. (c) Wang, F.; Nishimoto, Y.; Yasuda, M. Insertion of Diazo Esters into C–F Bonds toward Diastereoselective One-Carbon Elongation of Benzylic Fluorides: Unprecedented BF₃ Catalysis with C–F Bond Cleavage and Reformulation. *J. Am. Chem. Soc.* **2021**, *143*, 20616–20621.
- (17) See [Supporting Information](#) for further details.
- (18) Bickelhaupt, F. M.; Houk, K. N. Analyzing Reaction Rates with the Distortion/Interaction-Activation Strain Model. *Angew. Chem., Int. Ed.* **2017**, *56*, 10070–10086.
- (19) (a) Horn, P. R.; Head-Gordon, M. Polarization Contributions to Intermolecular Interactions Revisited with Fragment Electric-Field Response Functions. *J. Chem. Phys.* **2015**, *143*, No. 114111. (b) Horn, P. R.; Mao, Y.; Head-Gordon, M. Defining the Contributions of Permanent Electrostatics, Pauli Repulsion, and Dispersion in Density Functional Theory Calculations of Intermolecular Interaction Energies. *J. Chem. Phys.* **2016**, *144*, No. 114107. (c) Horn, P. R.; Mao, Y.; Head-Gordon, M. Probing Non-Covalent Interactions with a Second

Generation Energy Decomposition Analysis Using Absolutely Localized Molecular Orbitals. *Phys. Chem. Chem. Phys.* **2016**, *18*, 23067.

(20) Salwiczek, M.; Nyakatura, E. K.; Gerling, U. I. M.; Ye, S.; B Koks, B. Fluorinated Amino Acids: Compatibility with Native Protein Structures and Effects on Protein-Protein Interactions. *Chem. Soc. Rev.* **2012**, *41*, 2135–2171.

(21) Ohshima, T.; Shibasaki, M. Catalytic Asymmetric Epoxidation of α,β -Unsaturated Amides: Efficient Synthesis of β -Aryl α -Hydroxy Amides Using a One-Pot Tandem Catalytic Asymmetric Epoxidation–Pd-Catalyzed Epoxide Opening Process. *J. Am. Chem. Soc.* **2002**, *124*, 14544–14545.